Sensor and Simulation Notes

Note 399

1 May 1996

Discrete and Continuous E-Plane Bends in Parallel-Plate Waveguide

Carl E. Baum
Phillips Laboratory

Abstract

Discrete bends in the propagation direction of plane TEM waves can be achieved utilizing the Brewster angle at a planar interface between media of different uniform isotropic permittivities. This paper extends this to cases of multiple dielectric or nonuniform permittivity. The nonuniform case is a generalization of the Brewster-angle concept. This is also related to special log-spiral solutions of the general differential-geometry equations for synthesis of two-dimensional transient lenses for propagating TEM waves.

1. Introduction

A recent paper [2] has considered the design of two-dimensional lenses, the geometry being independent of the z coordinate, the direction of the magnetic field. Constraining the permeability μ to be uniform, scalar, positive, and frequency-independent (e.g., μ_0), the permittivity ε is allowed to be nonuniform (i.e., spatially variable), but still scalar, positive, and frequency independent. In that paper, a solution technique for the synthesis of such lenses has been developed, utilizing a conformal transformation as an intermediate step for generating the required (u_1, u_2, u_3) orthogonal curvilinear coordinate system. A specific example of an E-plane bend was also exhibited.

The present paper generalizes some of the previous results. As before, the electric field is in the u_1 direction, the magnetic field is in the u_2 direction, and propagation is in the u_3 direction to give a TEM wave and simplify the form of the differential-geometry equations. The appendices develop a general form of solution which includes a class of log-spiral solutions, as well as the E-plane bend (azimuthal propagation) in [2], and the complementary case of cylindrical-radial propagation. A particular choice of a parameter in the log-spiral solutions gives a case in which the permittivity is constant along certain planes (planes of constant azimuth ϕ). This is related to the Brewster-angle phenomenon for the total transmission of plane waves between two media of different uniform permittivities meeting at a planar interface.

After considering the simpler case of a jacket in which the perfectly conducting guiding sheets are closely spaced in terms of wavelength (Section 2), the Brewster angle is used to give discrete bends (Section 3) at one or more such interfaces. Continuing on to small changes in permittivity (Section 4), differential equations for continuous variation of permittivity are developed, allowing various combinations of uniform and nonuniform permittivity. This is then tied to the special log-spiral solutions (Section 5).

2. Solution for Closely Spaced, Perfectly Conducting Sheets Bounding an Isotropic Inhomogeneous Dielectric Medium

A jacket [4, 5] is a kind of two-dimensional space for the propagation of electromagnetic waves. The assumed form of our TEM wave is uniform in terms of the formal fields (primed quantities in terms of which the u_n coordinates are like Cartesian coordinates). The assumed wave is then like

$$\vec{E} = E_1 \vec{1}_1 = \frac{E_0'}{h_1} f\left(t - \frac{u_3}{c'}\right) \vec{1}_1$$
$$\vec{H} = H_2 \vec{1}_2 = \frac{E_0'}{h_2 Z_0'} f\left(t - \frac{u_3}{c'}\right) \vec{1}_2 \tag{2.1}$$
$$c' = [\mu' \varepsilon']^{-\frac{1}{2}} \quad , \quad Z_0' = \left[\frac{\mu'}{\varepsilon'}\right]^{\frac{1}{2}} \quad , \quad \mu' = \mu \quad , \quad \varepsilon' = \varepsilon_{\min}$$

with μ' and ε' as real and positive constants. For present purposes our jacket is taken as the space between two closely spaced (but, in general, curved) perfectly conducting sheets with the dielectric region (variable scalar permittivity ε, constant scalar permeability μ) defined by

$$u_1^{(1)} \le u \le u_1^{(2)} \tag{2.2}$$

the superscripts indicating the two perfectly conducting boundaries. In addition we take the jacket to be independent of the z coordinate with

$$u_2 = z \quad , \quad \vec{1}_2 = \vec{1}_z \quad , \quad h_2 = 1 \tag{2.3}$$

so that propagation and the electric-field orientation are orthogonal to the z axis. This type of jacket is simpler than the body-of-revolution type in [4] due to the constant h_2 in the present case. (See Appendix A and [5] for more detailed discussion of the coordinates, scaling relations, and constitutive parameters.) The spacing of the boundary sheets (in the $\vec{1}_1$ direction) is

$$h_\Delta = h_\Delta(u_2, u_3) = h_1 \Delta u_1 = h_3^{-1} \Delta u_1$$
$$\Delta u_1 \equiv u_1^{(2)} - u_1^{(1)} \tag{2.4}$$
$$h_3 = h_1^{-1} = \left[\frac{\varepsilon_{\min}}{\varepsilon}\right]^{\frac{1}{2}} \le 1$$

The spacing can be determined once ε has been specified.

Figure 2.1A shows the special case in which

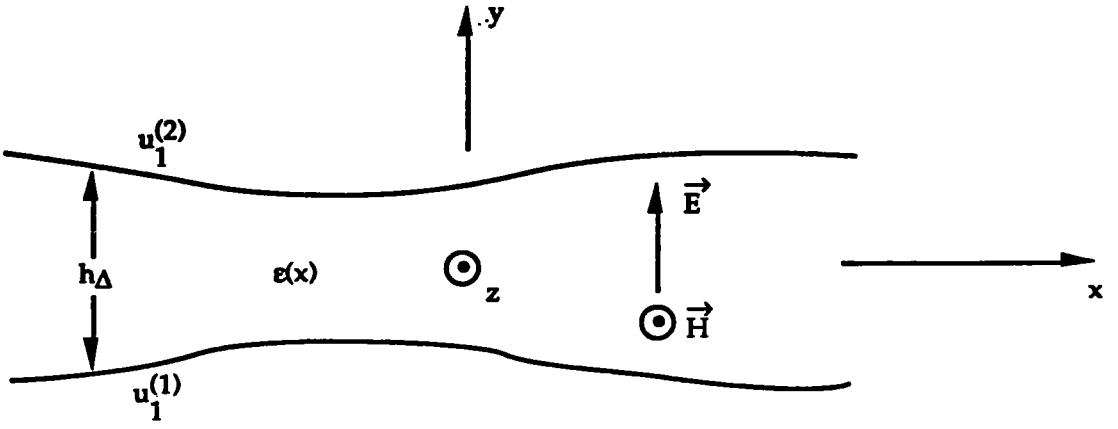

A. Straight jacket

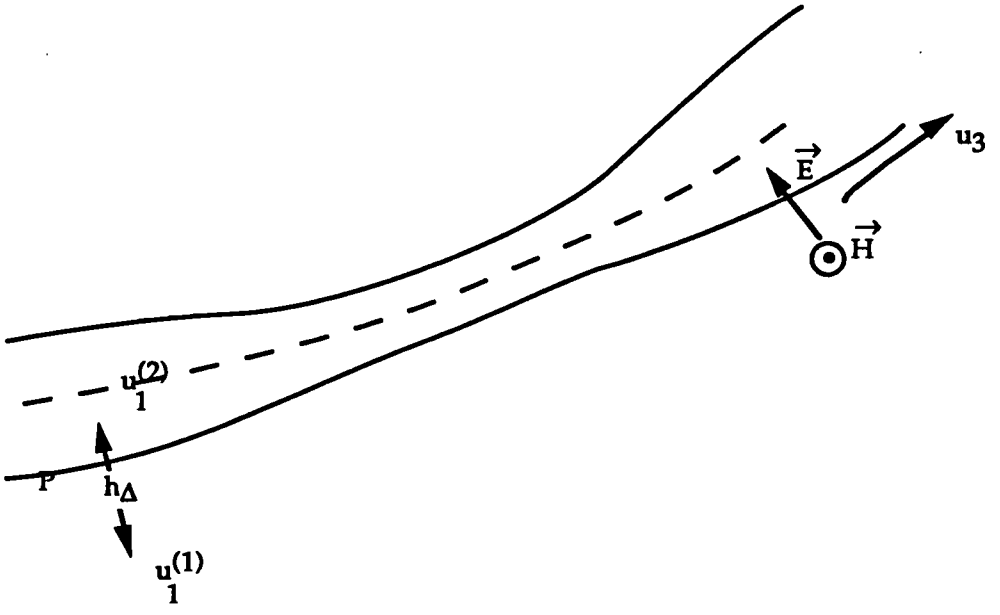

B. Bent (curved) jacket

Fig. 2.1. Closely Spaced Perfectly Conducting Sheets with Variable Spacing

$$\vec{1}_1 = \vec{1}_y \quad , \quad \vec{1}_3 = \vec{1}_x \tag{2.5}$$

which can be labeled a straight jacket. This simplifies matters as

$$u_3 = u_3(x) \quad , \quad h_3 = \left| \frac{dx}{du_3} \right| \tag{2.6}$$

Given some $\varepsilon(x)$, this can be integrated to give

$$u_3 = \int_0^x \frac{dx''}{h_3} = \int_0^x \left[\frac{\varepsilon(x'')}{\varepsilon_{\min}} \right]^{\frac{1}{2}} dx'' \tag{2.7}$$

with the integration constant (and sign) chosen for convenience. In turn, the boundary spacing can be found from (2.4).

Figure 2.1B shows a more general case of a bent or curved jacket where on a plane of constant z the u_3 coordinate can be defined along a path P midway between the two boundaries. In this case if one defines ℓ as the arc length along P (from some arbitrary starting point), then we have

$$\begin{aligned} &\varepsilon = \varepsilon(\ell) \quad , \quad u_3 = u_3(\ell) \\ &h_3^2 = \left(\frac{\partial x}{\partial u_3} \right)^2 + \left(\frac{\partial y}{\partial u_3} \right)^2 = \left(\frac{\partial \ell}{\partial u_3} \right)^2 \\ &u_3 = \int_0^\ell \frac{d\ell''}{h_3} = \int_0^\ell \left[\frac{\varepsilon(\ell'')}{\varepsilon_{\min}} \right]^{\frac{1}{2}} d\ell'' \end{aligned} \tag{2.8}$$

As discussed in [5] one can construct a lens from a set of jackets by stacking them in the $\vec{1}_1$ direction so that the boundaries of adjacent jackets have common boundaries $u_1^{(n)}$. However, if one is to now remove the boundaries, it is necessary that the u_3 coordinate be unchanged as one moves in the $\vec{1}_1$ direction (i.e., across such boundaries). This, in turn, places additional constraints on the coordinates and allowable distribution of ε. So now let us consider bends in lenses with TEM waves as in (2.1) and (2.3), but with the boundary spacing h_Δ no longer small so that variation with respect to u_1 is now allowed.

3. Discrete Bends

A basic bend geometry is indicated in fig. 3.1. A uniform TEM wave is incident from the left in a uniform medium of permittivity ε_1 and transmitted into the second medium with permittivity ε_2 as a uniform TEM wave provided certain Brewster-angle conditions are met [1], namely

$$\cos(\psi_{iB}) = \left[\frac{\varepsilon_1}{\varepsilon_2 + \varepsilon_1}\right]^{\frac{1}{2}} = \sin(\psi_{tB})$$

$$\sin(\psi_{iB}) = \left[\frac{\varepsilon_2}{\varepsilon_2 + \varepsilon_1}\right]^{\frac{1}{2}} = \cos(\psi_{tB})$$

$$\cot(\psi_{iB}) = \left[\frac{\varepsilon_1}{\varepsilon_2}\right]^{\frac{1}{2}} = \tan(\psi_{tB})$$

$$\psi_{iB} + \psi_{tB} = \frac{\pi}{2}$$

$$\psi_b = \psi_{iB} - \psi_{tB} \equiv \text{bend angle}$$

$$\sin(\psi_b) = \frac{\varepsilon_2 - \varepsilon_1}{\varepsilon_2 + \varepsilon_1}$$

$$\cos(\psi_b) = \frac{2[\varepsilon_2\varepsilon_1]^{\frac{1}{2}}}{\varepsilon_2 + \varepsilon_1}$$

$$\tan(\psi_b) = \frac{1}{2}\left[\left[\frac{\varepsilon_2}{\varepsilon_1}\right]^{\frac{1}{2}} - \left[\frac{\varepsilon_1}{\varepsilon_2}\right]^{\frac{1}{2}}\right] \qquad (3.1)$$

$$\frac{D_2}{D_1} = \left[\frac{\varepsilon_2}{\varepsilon_1}\right]^{\frac{1}{2}}$$

Figure 3.1 illustrates the case that ε is increasing to the right (increasing x) so that the plate spacing is also increasing to keep the transmission-line admittance per unit width the same, i.e.

$$Y_c' = \frac{Y_{wn}}{D_n} \quad , \quad n = 1,2$$

$$Y_{wn} = Z_{wn}^{-1} = \left[\frac{\varepsilon_n}{\mu}\right]^{\frac{1}{2}} \equiv \text{wave admittance of } n\text{th medium} \qquad (3.2)$$

The interface S between the two media has its surface normal inclined an angle ψ_{iB} with respect to the direction of incidence (the $\vec{1}_x$ direction). Note that there are two choices for the bend direction, up with

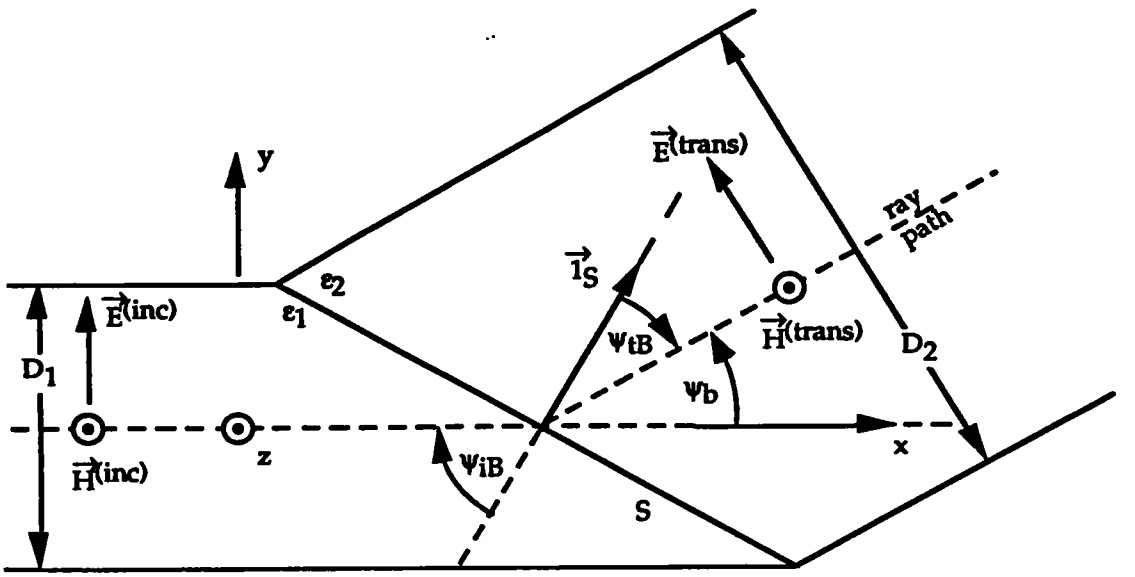

Fig. 3.1. Bend in Parallel-Plate Waveguide Utilizing Brewster Angle at Interface Between Two Uniform Media.

ψ_b positive for increasing ε (which we use here), or down (toward $-\vec{1}_y$). In the present case, S inclines from upper left to lower right, while the alternative has S inclining from lower left to upper right. Said another way the surface normal $\vec{1}_S$ pointing into the second medium points up from the x axis.

The incident field takes the form

$$\vec{E}^{(inc)} = E_y \vec{1}_y = E_0' f\left(t - \frac{x}{c_{w1}}\right)\vec{1}_y$$

$$\vec{H}^{(inc)} = H_z \vec{1}_z = \frac{E_0'}{Z_{w1}} f\left(t - \frac{x}{c_{w1}}\right)\vec{1}_z$$

$$Z_{wn} = \left[\frac{\mu}{\varepsilon_n}\right] \equiv \text{wave impedance of } n\text{th medium} \tag{3.3}$$

$$c_{wn} = [\mu\varepsilon_n]^{-\frac{1}{2}} \equiv \text{wave speed in } n\text{th medium}$$

in the first medium (permittivity ε_1). In passing into the second medium, the electric field creased by the factor D_1/D_2 (the magnetic field being unchanged), reoriented by a rotation of ψ_b, and propagates with the speed c_{w2}.

Applying this bend twice we have the configuration in fig. 3.2. Note the same "positive" orientation of the Brewster interfaces S_n (upper left to lower right). This can be applied to the case of N such bends with (3.1) applied to the nth bend as

$$\cot(\psi_{iBn}) = \left[\frac{\varepsilon_n}{\varepsilon_{n+1}}\right]^{\frac{1}{2}} = \tan(\psi_{tBn})$$

$$\sin(\psi_{bn}) = \frac{\varepsilon_{n+1} - \varepsilon_n}{\varepsilon_{n+1} + \varepsilon_n}$$

$$\frac{D_{n+1}}{D_n} = \left[\frac{\varepsilon_{n+1}}{\varepsilon_n}\right]^{\frac{1}{2}} \tag{3.4}$$

$$\frac{D_{n+1}}{D_1} = \left[\frac{\varepsilon_{n+1}}{\varepsilon_1}\right]^{\frac{1}{2}}$$

as well as other forms in (3.1) generalized by inspection. The illustration in fig. 3.2 is for the case of progressively increasing ε, i.e., $\varepsilon_1 < \varepsilon_2 < \varepsilon_3$. This need not be the case. For a decrease in ε on passing through S_n, the bend angle ψ_{bn} merely becomes negative.

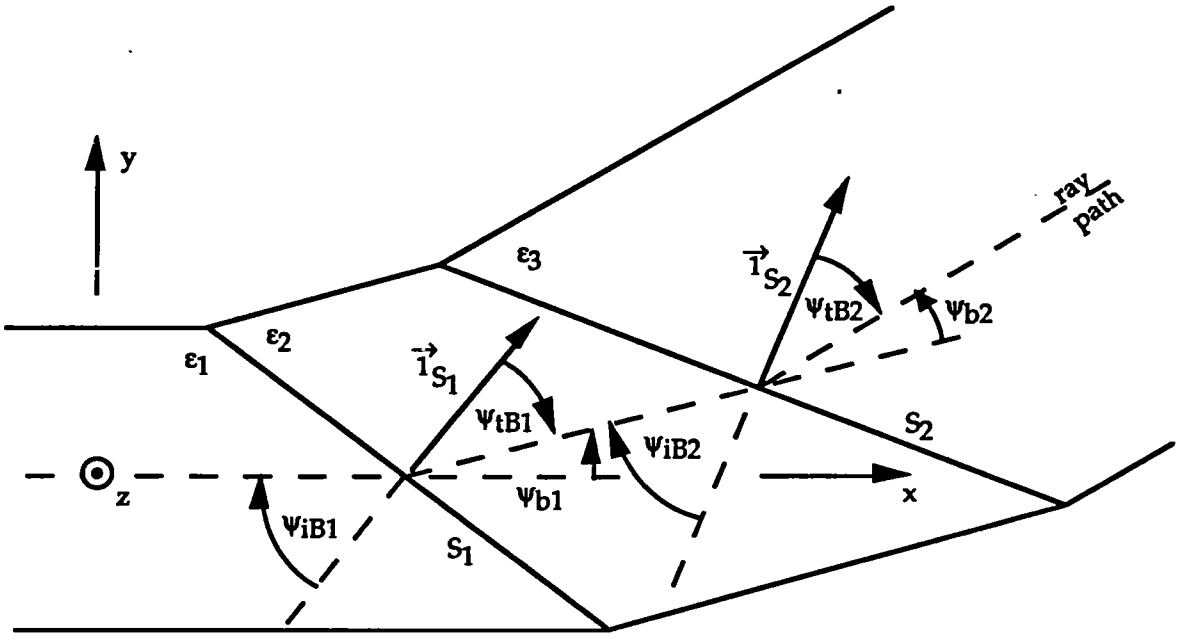

Fig. 3.2. Two Bends in the Same Direction with Two Brewster Interfaces.

By reversing the direction of inclination of one of the Brewster interfaces (S_2 in fig. 3.3) one can reverse the bend direction while progressively increasing the permittivity (as in $\varepsilon_1 < \varepsilon_2 < \varepsilon_2$ in fig. 3.3). With this reversal of bend direction, the formulae in (3.4) and (3.1) are still applicable. Defining

$$\Sigma_n = \begin{cases} +1 \text{ for positive inclination of } S_n \ (\vec{1}_{S_n} \text{ rotated in positive sense (counterclockwise) from ray path)} \\ -1 \text{ for "negative" inclination of } S_n \ (\vec{1}_{S_n} \text{ rotated in negative sense (clockwise) from ray path)} \end{cases} \tag{3.5}$$

the cumulative bend angle through the Nth Brewster interface is just

$$\psi_b^{(N)} = \sum_{n=1}^{N} \Sigma_n \psi_{bn} \tag{3.6}$$

This is measured positive with respect to $\vec{1}_x$, the direction of the initial ray path. If N is the total number of such interfaces, this represents the total bend angle.

A special case has a zero total bend angle, i. e., the wave in the N + 1st region propagates parallel to $\vec{1}_x$. For the case of N = 2 as in fig. 3.3, this implies

$$\begin{aligned} \psi_{b1} &= \psi_{b2} \\ \frac{\varepsilon_3}{\varepsilon_2} &= \frac{\varepsilon_2}{\varepsilon_1} \end{aligned} \tag{3.7}$$

So, given the initial and final permittivities, the intermediate permittivity is required to be the geometric mean.

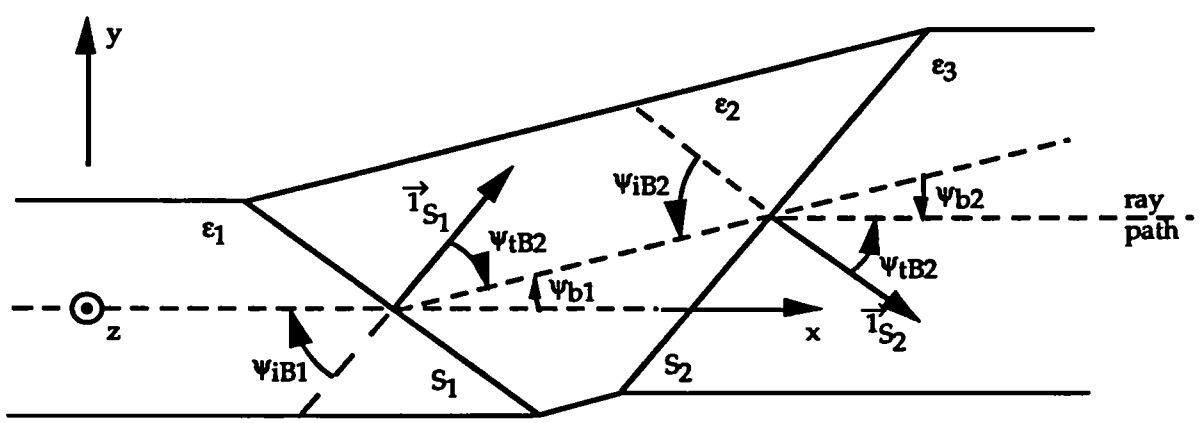

Fig. 3.3. Two Bends in Opposite Directions with Progressively Increasing Permittivity

4. Small Change in Bend Angle for Small Change in Permittivity

Preparing for a later continuous spatial variation of the permittivity, let us first consider the case of a small change in permittivity in crossing a Brewster interface S as previously illustrated in fig. 3.1. Setting

$$\varepsilon_1 \equiv \varepsilon \quad , \quad \varepsilon_2 \equiv \varepsilon + \Delta\varepsilon \tag{4.1}$$

then from (3.1) we have

$$\tan(\psi_{iB}) = \left[1+\frac{\Delta\varepsilon}{\varepsilon}\right]^{\frac{1}{2}} = \cot(\psi_{tB}) \tag{4.2}$$

$$\lim_{\Delta\varepsilon\to 0} (\psi_{iB}) = \lim_{\Delta\varepsilon\to 0} \psi_{tB} = \frac{\pi}{4}$$

so small changes of ε are associated with a Brewster angle of $\pi/4$. For convenience we define a dimensionless relative permittivity

$$\varepsilon_r \equiv \frac{\varepsilon}{\varepsilon_{ref}} \tag{4.3}$$

$\varepsilon_{ref} \equiv$ convenient reference permittivity (e.g., ε_0 or some starting ε)

Continuing the development we write

$$\psi_{iB} = \frac{\pi}{4} + \Delta\psi_{iB} \quad , \quad \psi_{tB} = \frac{\pi}{4} + \Delta\psi_{tB}$$

$$\Delta\psi_{tB} = -\Delta\psi_{iB} \tag{4.4}$$

$$\Delta\psi_b = \Delta\psi_{iB} - \Delta\psi_{tB} = 2\Delta\psi_{iB} \text{ (small bend angle)}$$

Then expand the various functions as

$$\tan\left(\frac{\pi}{4} + \Delta\psi_{iB}\right) = \tan\left(\frac{\pi}{4}\right) + \sec^2\left(\frac{\pi}{4}\right)\Delta\psi_{iB} + O\left((\Delta\psi_{iB})^2\right)$$

$$= 1 + 2\Delta\psi_{iB} + O\left((\Delta\psi_{iB})^2\right) \text{ as } \Delta\psi_{iB}\to 0 \tag{4.5}$$

$$\left[1 + \frac{\Delta\varepsilon_r}{\varepsilon_r}\right]^{\frac{1}{2}} = 1 + \frac{1}{2}\frac{\Delta\varepsilon_r}{\varepsilon_r} + O\left(\left(\frac{\Delta\varepsilon_r}{\varepsilon_r}\right)^2\right) \text{ as } \frac{\Delta\varepsilon_r}{\varepsilon_r}\to 0$$

So to first order we have

$$\Delta\psi_{iB} = \frac{1}{4}\frac{\Delta\varepsilon_r}{\varepsilon_r} = \frac{1}{2}\Delta\psi_b = -\Delta\psi_{tB} \tag{4.6}$$

Taking the limit gives derivatives as

$$\begin{aligned}\frac{d\psi_{iB}}{d\varepsilon} &= -\frac{d\psi_{tB}}{d\varepsilon} = \frac{1}{2}\frac{d\psi_b}{d\varepsilon} = \frac{1}{4\varepsilon} \\ \frac{d\psi_{iB}}{d\ell n(\varepsilon)} &= -\frac{d\psi_{tB}}{d\ell n(\varepsilon)} = \frac{1}{2}\frac{d\psi_b}{d\ell n(\varepsilon)} = \frac{1}{4}\end{aligned} \tag{4.7}$$

If this change occurs with respect to a change in some other parameter, say arc length $d\ell$, we have

$$\frac{d\psi_{iB}}{d\ell} = -\frac{d\psi_{tB}}{d\ell} = \frac{1}{2}\frac{d\psi_b}{d\ell} = \frac{1}{4}\frac{d\ell n(\varepsilon)}{d\ell} \tag{4.8}$$

This is integrable giving a cumulative change in the angles. Expressing this for the bend angle along some ray path P with arc parameter ℓ (or other parameter if one chooses) from some initial set of parameters (subscript 1) we have

$$\psi_b - \psi_{b1} = \frac{1}{2}\left[\ell n(\varepsilon_r) - \ell n(\varepsilon_{r1})\right] = \frac{1}{2}\ell n\left(\frac{\varepsilon_r}{\varepsilon_{r1}}\right) \tag{4.9}$$

Comparing this to the formulae for a set of discrete bends in (3.1) and (3.6), one can see that the results are somewhat different. However, (4.9) can be considered a limiting case for large N and small $\Delta\varepsilon$ at each of the N Brewster interfaces. Along this ray path P the u_3 coordinate monotonically increases (Appendix A). Writing

$$\varepsilon_r \equiv \varepsilon_{\min} \quad , \quad \varepsilon_r = \varepsilon_r(\ell) \tag{4.10}$$

we have from (A.11)

$$\begin{aligned} &h_3 = \varepsilon_r^{\frac{1}{2}}(\ell) \quad \text{(scale factor for } u_3 \text{ coordinate)} \\ &u_3 = \int_{\ell_1}^{\ell}\frac{d\ell'}{h_3(\ell')} = \int_{\ell_1}^{\ell}\varepsilon_r^{\frac{1}{2}}(\ell')\,d\ell' \end{aligned} \tag{4.11}$$

with the integral along P. This relates to the later consideration (next section) of the continuous case from differential-geometry considerations. Note that the ray path P can also be generated from (4.9). If the initial direction is specified by, say $\psi_{b1} = 0$, we then have

$$\psi_b(\ell) = \frac{1}{2}\ell n\left(\frac{\varepsilon_r(\ell)}{\varepsilon_r(\ell_1)}\right) = \arctan\left(\frac{dy}{dx}\right) \tag{4.12}$$

So at any position along P, the slope of this path is given in terms of parameters from previous positions along the path.

In a general lens design one needs to consider not only a single ray path, but also other ray paths and how the ensemble of paths works together to allow TEM waves to propagate with a common dependence on the propagation coordinate u_3 with the electric field in the orthogonal u_1 direction (Appendix A). Here we consider a limitation on the allowable spatial region for the lens (the lens domain) based on a spatial singularity.

Consider fig. 4.1 along with fig. 3.2 for some of the other symbols. On passing through S_1 the ray path P is bent positive $\Delta\psi_{b1}$ and another $\Delta\psi_{b2}$ on passing through S_2. The relative permittivity increases by $\Delta\varepsilon_{r1}$ and another $\Delta\varepsilon_{r2}$ on passing through these two surfaces. all these changes are assumed small (so fig. 4.1 is not to scale). The distance along P between S_1 and S_2 is $\Delta\ell$ (also small). With S_1 and S_2 nearly parallel ($\Delta\psi_{b2}$ being small) the perpendicular distance between S_1 and S_2 near the ray path is $\Delta\ell/\sqrt{2}$ since ψ_{tB1} is $\pi/4$ (in the limit). Assuming continuous derivatives we have

$$\Delta\psi_{b2} \simeq \Delta\psi_{b1} \simeq \Delta\psi_b \quad , \quad \Delta\varepsilon_{r1} \simeq \Delta\varepsilon_{r2} \simeq \Delta\varepsilon_r \tag{4.13}$$

where S_1 and S_2 can be taken as any two nearby such surfaces for continuously varying ε_r. The two Brewster surfaces S_1 and S_2 intersect in a line (parallel to the z axis) designated P_s. The distance along these surfaces (a slant distance) from the ray path is

$$d_{s1} \simeq d_{s2} \simeq \frac{\Delta\ell}{\sqrt{2}\Delta\psi_b} = \sqrt{2}\,\frac{\varepsilon_r \Delta\ell}{\Delta\varepsilon_r} \tag{4.14}$$

Taking the limit as $\Delta\ell \to 0$ we have

$$d_s = \frac{1}{\sqrt{2}}\frac{d\ell}{d\psi_b} = \sqrt{2}\varepsilon_r \frac{d\ell}{d\varepsilon_r} = \sqrt{2}\,\frac{d\ell}{d\ell n(\varepsilon_r)} \tag{4.15}$$

Since the permittivity increases (or decreases) in a direction normal to each $\vec{1}_S$, this direction being at an angle of $\pi/4$ from the ray path, we also have

$$d_s^{-1} = \frac{1}{\sqrt{2}}\frac{d\ell n(\varepsilon_r)}{d\ell} = \frac{1}{2}\vec{1}_S \cdot \nabla \ell n(\varepsilon_r) \tag{4.16}$$

Note that if ε_r decreases along the ray path the sign of d_s can become negative corresponding to a flip of the position of P_s from upper left to lower right in fig. 3.1. As one progresses along the ray path P, the length of d_s can vary. The lens domain should not include singularities such as P_s. As such the perfectly

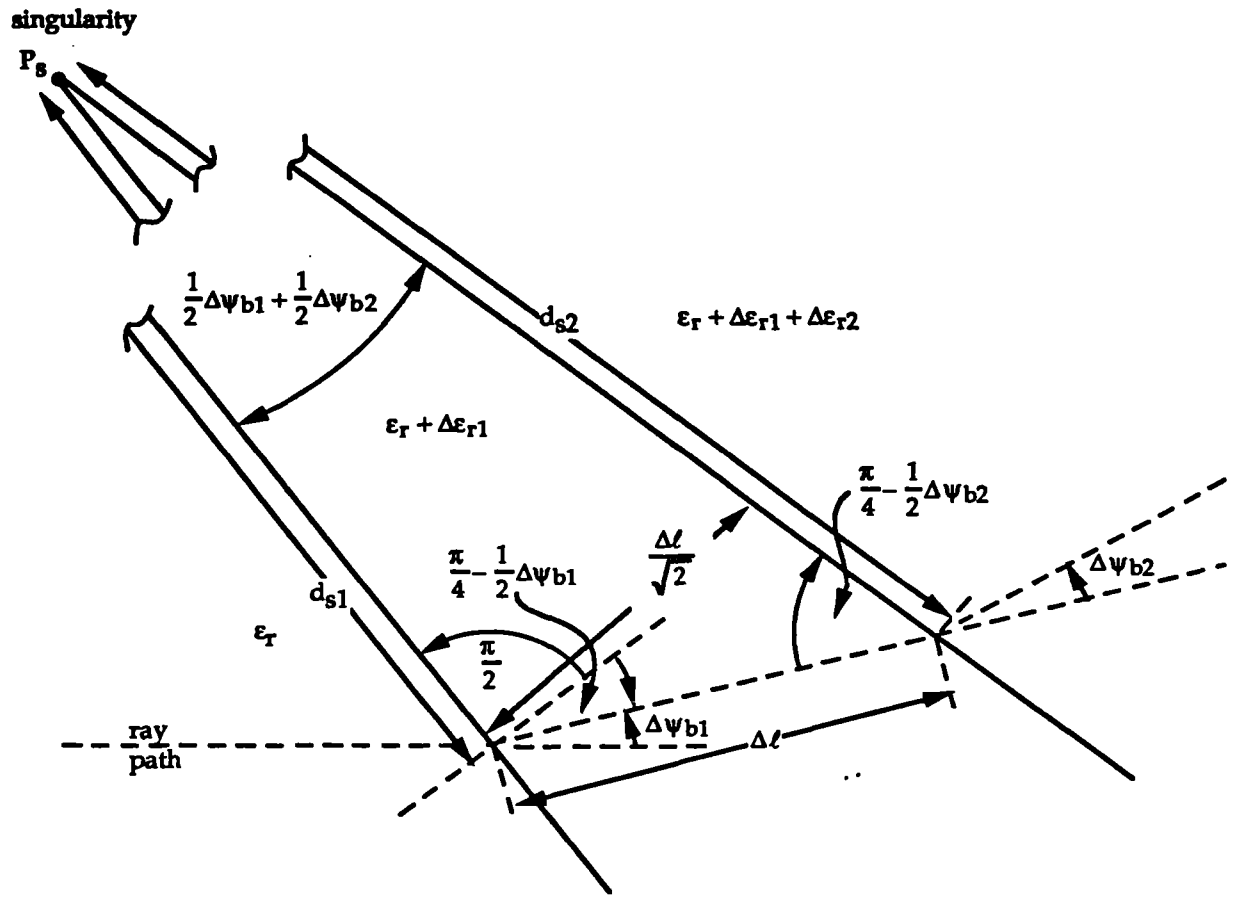

Fig. 4.1. Spatial Singularity Associated with Turning of Ray Path

conducting electric boundaries ($u_1^{(1)}$ and $u_1^{(2)}$ in Section 2) need to be chosen to exclude such positions from the lens domain. Note from the above that more rapidly varying $\ell n(\varepsilon_r)$ gives smaller $|d_s|$ and hence a more restricted lens domain.

As discussed in this section, we have a constructive way to design this kind of lens. Basically it involves the discrete procedure in Section 2 generalized to a continuous various of ε_r. A set of steps for this is:

1. Specify a ray path P in the x,y plane.

2. At each point of P find ψ_b from the slope and $d\psi_b / d\ell$ (the curvature).

3. With some starting value of ε_r find $\varepsilon_r(\ell)$ from (4.15) by integrating along P.

4. Add $\pi/4$ to ψ_b to give $\vec{1}_S$ and assign the value of ε_r at this position on ℓ everywhere along the surface S. Repeat for all positions on P to determine ε_r in the x,y plane.

5. Go to another position in the lens domain and find another ray path starting in a direction with angle $-\pi/4$ from the surface normal to local S, i.e., ψ_b as one passes through successive surfaces S (or S_n if one prefers).

6. Take two such ray paths to define the lens domain as the region between them, taking care to use such a pair of paths that have no singularities "between" them. Note that the ray paths need not extend to infinity but can be truncated as convenient. Place conducting sheets on these two ray paths extended in the $\pm z$ directions as surfaces.

If one wishes, such a continuous solution can be matched to two regions of uniform ε_r (as in Section 2) to "begin" and "end" the lens at two convenient choices of S. This might correspond to connection to uniform transmission lines, sources, terminations, radiating antenna apertures, etc. This can be extended to a wide variety of combinations of continuous nonuniform regions with uniform regions.

5. Special Log-Spiral Solutions

Appendix C treats a general class of log-spiral solutions based on the differential-geometry equations for two-dimensional TEM waves in Appendix A and a general class of solutions in Appendix B. Here we consider log-spiral solutions consistent with the continuous variation of permittivity in Section 4.

In (C.10) for the permittivity there is a parameter (an angle) a' which can be selected at our convenience. Two simple special cases, azimuthal and radial propagation, are associated with $a' = \pi/2$ and $a' = 0$, respectively, in Appendix D. Here we choose $a' = \pi/4$ which gives

$$\frac{\varepsilon}{\varepsilon_{\min}} = \frac{h_1}{h_3} = e^{2\phi} \ , \phi \geq 0 \tag{5.1}$$

Noting that constant ϕ is a straight line in the complex plane (A.13) given by

$$\zeta = x + jy = \Psi e^{j\phi} \tag{5.2}$$

we can identify the planes of constant ϕ in three-dimensional space as Brewster surfaces designated S or S_n in Sections 3 and 4.

The solution uses the complex coordinates (a conformal transformation of ζ)

$$\begin{aligned} v(\zeta) &\equiv v_3(\zeta) + jv_1(\zeta) \\ v_1 &= \frac{1}{\sqrt{2}a}\left[-\ell n(a\Psi) + \phi\right] \\ v_3 &= \frac{1}{\sqrt{2}a}\left[\ell n(a\Psi) + \phi\right] \\ h_v &= \left|\frac{d\zeta}{dv}\right| = a\Psi \ , \ a \equiv \text{ positive scaling constant} \end{aligned} \tag{5.3}$$

Other parameters are

$$h_1 = \left|\frac{dv_1}{du_1}\right| h_v = a\Psi e^{\sqrt{2}av_1} = e^{\ell n(a\Psi) + \sqrt{2}av_1} = e^{\phi}$$

$$h_2 = 1$$

$$h_3 = \left|\frac{dv_3}{du_3}\right| h_v = a\Psi e^{-\sqrt{2}av_1} = e^{\ell n(a\Psi) - \sqrt{2}av_3} = e^{-\phi}$$

$$c_w = [\mu\varepsilon]^{-\frac{1}{2}} \quad c' = e^{-\phi}c' \equiv \text{local wave speed}$$

$$c' = [\mu\varepsilon_{\min}]^{-\frac{1}{2}}$$

$$Z_w = \left[\frac{\mu}{\varepsilon}\right]^{-\frac{1}{2}} = e^{-\phi}Z_0' \equiv \text{local wave impedance} \tag{5.4}$$

$$Z_0' = \left[\frac{\mu}{\varepsilon_{\min}}\right]^{-\frac{1}{2}}$$

The (u_1, u_2, u_3) orthogonal curvilinear coordinates are

$$\begin{aligned} u_1 &= -\frac{1}{\sqrt{2}a}e^{-\sqrt{2}av_1} = -\frac{1}{\sqrt{2}a}e^{\ell n(a\Psi)-\phi} = -\frac{1}{\sqrt{2}}\Psi e^{-\phi} \\ u_2 &= z \\ u_3 &= \frac{1}{\sqrt{2}a}e^{\sqrt{2}av_3} = \frac{1}{\sqrt{2}a}e^{\ell n(a\Psi)+\phi} = \frac{1}{\sqrt{2}}\Psi e^{\phi} \end{aligned} \tag{5.5}$$

The electric boundaries are given by two choices of u_1 (say $u_1^{(1)}$ and $u_1^{(2)}$) giving logarithmic spirals as in (5.4). Constant arrival-time surfaces (or constant phase surfaces) are given by constant u_3 which are also logarithmic spirals. This is illustrated in fig. 5.1.

The TEM wave is given by

$$\begin{aligned} \vec{E} &= E_1 \vec{1}_1 = \frac{E_0'}{h_1} f\left(t - \frac{u_3}{c'}\right)\vec{1}_1 = E_0' e^{-\phi} f\left(t - \frac{u_3}{c'}\right)\vec{1}_1 \\ \vec{H} &= H_2 \vec{1}_2 = \frac{E_0'}{Z_0'} f\left(t - \frac{u_3}{c'}\right)\vec{1}_2 \end{aligned} \tag{5.6}$$

The various directions are given by the unit vectors

$$\begin{aligned} \vec{1}_1 &= \frac{\nabla u_1}{|\nabla u_1|} = \frac{1}{\sqrt{2}}\left[-\vec{1}_\Psi + \vec{1}_\phi\right] \\ \vec{1}_2 &= \vec{1}_z \\ \vec{1}_3 &= \frac{\nabla u_3}{|\nabla u_3|} = \frac{1}{\sqrt{2}}\left[\vec{1}_\Psi + \vec{1}_\phi\right] \end{aligned} \tag{5.7}$$

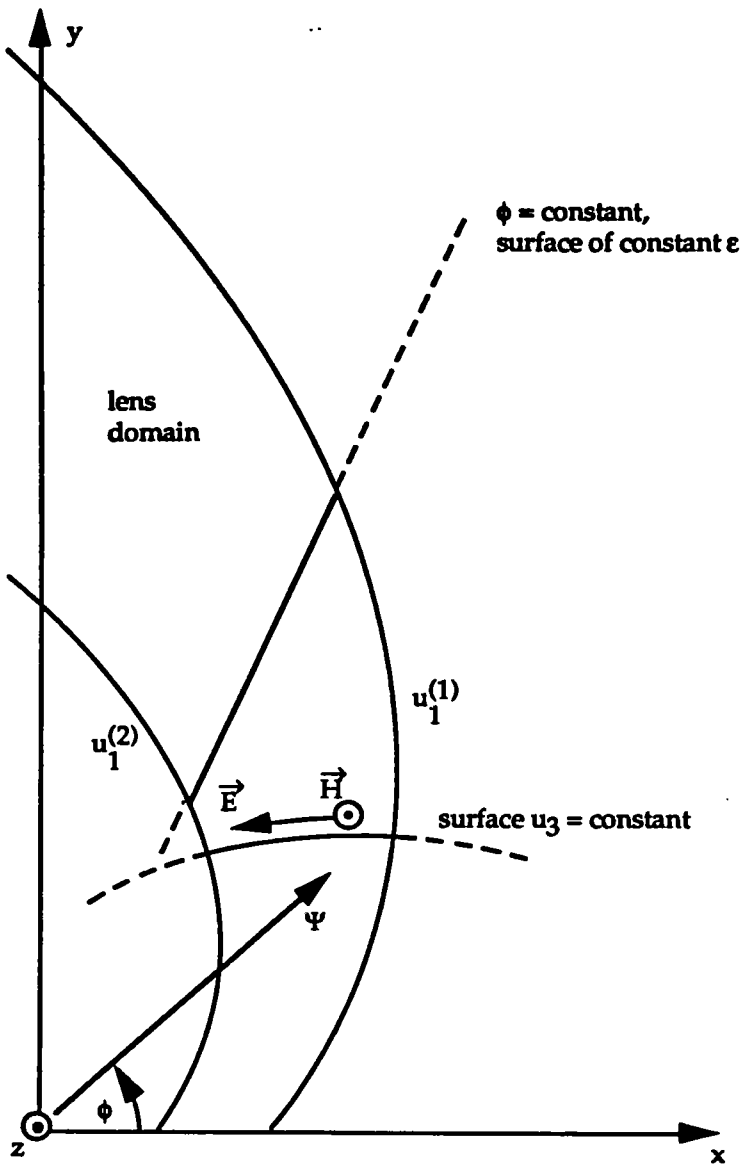

Fig. 5.1. Log-Spiral Lens

this shows that the direction of propagation $\vec{1}_3$ is oriented at an angle of $-\pi/4$ with respect to the constant-ϕ surfaces (Brewster surfaces) with surface normal $\vec{1}_\phi$. Furthermore, (5.6) shows that on such surfaces the magnitude of the electric field is constant for constant retarded time $t - u_3/c'$, consistent with Sections 3 and 4.

6. Concluding Remarks

There are various ways to approach the design of two-dimensional transient lenses with constant μ and variable ε. For small spacing of the conducting sheets, a jacket approach gives a very flexible design in which the variation of ε with u_3 can be specified along a planar curved path and the variable conductor spacing then computed. For large spacing of the conducting sheets (compared to local wavelengths at the highest frequencies of interest) this u_1 coordinate (in the electric-field direction) becomes important.

For electrically large Δu_1 one can approach this problem from both discrete and continuous points of view. The discrete approach relies on the Brewster-angle phenomenon of no reflection at a planar surface between adjacent regions of different permittivities. This can be repeated at some set of such interfaces to achieve various bend angles for the direction of propagation and various combinations of initial and final permittivities.

From a continuous point of view one can search for solutions of the differential-geometry equations to synthesize the (u_1 , u_3) coordinates (with u_2 = z). Here we have found a class of log-spiral solutions which, for a particular convenient choice of parameters, gives a special form in which constant ε occurs on planes of constant ϕ which can be interpreted as Brewster-angle interfaces for small change in ε, thereby giving a continuous variation of ε which corresponds to the discrete form. This also allows a lens design which contains both uniform- and variable-ε portions.

Further generalizations are possible. The particular log-spiral solution with constant-ϕ planes as planes of constant ε can be matched to a second such solution on some particular plane, say $\phi = \phi_p$, where the second solution has a different coordinate origin. This can be extended to some set of such matching planes (say M-1) where the M regions so defined all have different coordinate origins. Of course, one can then consider what happens as $M \to \infty$.

Besides log-spiral solutions the results of Appendix B allow a quadratic term in the exponential. This leads to coordinates based on the error function and Dawson's integral. So future investigations may lead to various additional types of two-dimensional transient lenses.

Appendix A. Summary of Two-Dimensional Differential-Geometry Lens Equations for Single Field Components

A lens with the constraints (2.3) that

$$u_2 = z\,,\ \vec{1}_2 = \vec{1}_z\,,\ h_2 = 1 \tag{A.1}$$

reduces the differential-geometry lens design to a two-dimensional problem (the lens being independent of one coordinate). Summarizing from [2,5] we have

$$\begin{aligned} h_n^2 &= \left(\frac{\partial x}{\partial u_n}\right)^2 + \left(\frac{\partial y}{\partial u_n}\right)^2 \quad \text{for } n = 1,3 \ \text{(scale factors)} \\ (d\ell)^2 &= \sum_{n=1}^{3} h_n^2 (du_n)^2 \quad \text{(line element)} \end{aligned} \tag{A.2}$$

The TEM formal fields are constrained to have the form

$$\begin{aligned} \vec{E}' &= E_1' \vec{1}_1 = E_0' f\left(t - \frac{u_3}{c'}\right)\vec{1}_1 \\ \vec{H}' &= H_2' \vec{1}_2 = \frac{E_0'}{Z_0'} f\left(t - \frac{u_3}{c'}\right)\vec{1}_2 \\ c' &= [\mu'\varepsilon']^{-\frac{1}{2}} \quad , \quad Z_0' = \left[\frac{\mu'}{\varepsilon'}\right]^{\frac{1}{2}} \end{aligned} \tag{A.3}$$

giving the physical fields (V/m and A/m)

$$\begin{aligned} \vec{E} &= E_1 \vec{1}_1 \quad , \quad E_1 = \frac{E_1'}{h_1} \\ \vec{H} &= H_2 \vec{1}_2 \quad , \quad H_2 = H_z = H_2' \end{aligned} \tag{A.4}$$

For this restricted form of the fields (one component each of electric and magnetic fields) the constitutive-parameter scaling reduces to

$$\mu' = h_1 h_3 \mu \quad , \quad \varepsilon' = \frac{h_3}{h_1}\varepsilon \tag{A.5}$$

Restricting to the case of uniform permeability we choose for convenience

$$\mu \equiv \mu' \geq \mu_0 \tag{A.6}$$

giving

$$h_1 h_3 = 1$$

$$\varepsilon = \frac{h_1}{h_3}\varepsilon' = h_3^{-2}\varepsilon' = h_1^2\varepsilon' \tag{A.7}$$

The local wave speed and wave impedance are

$$c_w = [\mu\varepsilon]^{-\frac{1}{2}} = \left[\frac{\varepsilon'}{\varepsilon}\right]^{\frac{1}{2}} c' = h_3 c'$$

$$Z_w = \left[\frac{\mu}{\varepsilon}\right]^{\frac{1}{2}} = \left[\frac{\varepsilon'}{\varepsilon}\right]^{\frac{1}{2}} Z_0' = h_3 Z_0' \tag{A.8}$$

Restricting (for causality)

$$\varepsilon \geq \varepsilon_{\min} \geq \varepsilon_0 \tag{A.9}$$

let us set

$$\varepsilon_{\min} \equiv \varepsilon' \tag{A.10}$$

which in turn restricts

$$h_3 = h_1^{-1} = \left[\frac{\varepsilon_{\min}}{\varepsilon}\right]^{\frac{1}{2}} \leq 1 \tag{A.11}$$

Note that the fields are related by

$$\frac{E_1}{H_2} = h_1^{-1} Z_0' = h_3 Z_0' = Z_w \tag{A.12}$$

consistent with the TEM nature of the assumed wave.

A convenient intermediate step, discussed in [2], for constructing the remaining u_1 and u_3 coordinates uses a conformal transformation

$$v(\zeta) \equiv v_3(\zeta) + jv_1(\zeta)$$

$$\zeta \equiv x + jy \text{ (complex coordinates)} \tag{A.13}$$

where $v(\zeta)$ is an analytic function. The line element is

$$|d\zeta|^2 = (dx)^2 + (dy)^2 = h_v^2 |dv|^2$$

$$h_v = \left|\frac{d\zeta}{dv}\right| \tag{A.14}$$

$$h_v^2 = h_{v_n}^2 = \left(\frac{\partial x}{\partial v_n}\right)^2 + \left(\frac{\partial y}{\partial v_n}\right)^2 \quad \text{for } n = 1,3$$

Lines of constant v_1 and v_3 (on a plane of constant z) form curvilinear squares (for equal decrements of v_1 and v_3). While the v_1, v_3 coordinates do not satisfy (A.7), except for the trivial case of $h_v = 1$, one can construct the corresponding u_n coordinates in the form

$$u_1 = u_1(v_1) \quad , \quad u_3 = u_3(v_3) \tag{A.15}$$

Then we have

$$h_n^2 = \left(\frac{\partial x}{\partial u_n}\right)^2 + \left(\frac{\partial y}{\partial u_n}\right)^2 = \left(\frac{dv_n}{du_n}\right)^2 \left[\left(\frac{\partial x}{\partial v_n}\right)^2 + \left(\frac{\partial y}{\partial v_n}\right)^2\right]$$

$$h_n = \left|\frac{dv_n}{du_n}\right| h_v \quad \text{for } n = 1,3 \tag{A.16}$$

which gives

$$h_1 h_3 = \left|\frac{dv_1}{du_1}\right| \left|\frac{dv_3}{du_3}\right| h_v^2 = 1 \tag{A.17}$$

This allows one to choose the v_n, giving the shape of constant v_1 and v_3 lines, and hence constant u_1 and u_3 lines, and solve for the u_1 and u_3 coordinates subject to the separability conditions in (A.15).

Appendix B. A General Class of Two-Dimensional Solutions

Consider some possible forms that the conformal transformation $v(\zeta)$ in (A.13) can take. Rewriting from (A.17)

$$\left|\frac{du_1}{dv_1}\right|\left|\frac{du_3}{dv_3}\right| = h_v^2 \tag{B.1}$$

the separability conditions (A.15) require that h_v can be factored as

$$\begin{aligned} h_v^2 &= \left|\frac{d\zeta}{dv}\right|^2 = \left|\frac{du_1}{dv_1}\right|\left|\frac{du_3}{dv_3}\right| \\ &= \left|\begin{array}{c}\text{real function} \\ \text{of } v_1 \text{ only}\end{array}\right|\left|\begin{array}{c}\text{real function} \\ \text{of } v_3 \text{ only}\end{array}\right| \end{aligned} \tag{B.2}$$

This implies

$$\left(\frac{d\zeta}{dv}\right)^2 = \left[\begin{array}{c}\text{real function} \\ \text{of } v_1 \text{ only}\end{array}\right]\left[\begin{array}{c}\text{real function} \\ \text{of } v_3 \text{ only}\end{array}\right]\left[\begin{array}{c}\text{complex function of} \\ v_1 \text{ and } v_3 \text{ of magnitude 1}\end{array}\right] \tag{B.3}$$

which allows us to write

$$\ell n\left(\frac{d\zeta}{dv}\right) = \left[\begin{array}{c}\text{real function} \\ \text{of } v_1 \text{ only}\end{array}\right] + \left[\begin{array}{c}\text{real function} \\ \text{of } v_3 \text{ only}\end{array}\right] + \left[\begin{array}{c}\text{imaginery function} \\ \text{of } v_1 \text{ and } v_3\end{array}\right] \tag{B.4}$$

Now $d\zeta/dv$ is analytic, as is the logarithm away from zeros and singularities of $d\zeta/dv$. So try a series expansion as

$$\ell n\left(\frac{d\zeta}{dv}\right) = \sum_{n=0}^{\infty} a_n v^n = \sum_{n=0}^{\infty} a_n [v_3 + jv_1]^n \tag{B.5}$$

This is an expansion about $v = 0$, but it can easily be shifted to another origin as desired. Writing out the first several terms we have

$$
\begin{aligned}
\ell n\left(\frac{d\zeta}{dv}\right) = a_0 \quad & \text{(acceptable)} \\
+a_1[v_3 + jv_1] \quad & \text{(acceptable)} \\
+a_2\left[v_3^2 + j2v_3v_1 - v_1^2\right] \quad & \text{(acceptable provided } a_2 \text{ is real)} \\
+a_3\left[v_3^3 + j3v_3^2v_1 - 3v_3v_1^2 - jv_1^3\right] \quad & \text{(unacceptable)} \\
+\ldots \quad & \text{(unacceptable)}
\end{aligned}
\tag{B.6}
$$

Here we see that, by comparing the terms in this series to the sum in (B.4), the terms for $n \geq 3$ cannot be used (i.e., these $a_n = 0$) due to the mixed terms involving both v_3 and v_1 which cannot all be purely imaginary by appropriate choice of complex a_n.

So now we write

$$
\frac{d\zeta}{dv} = e^{a_0 + a_1 v + a_2 v^2} \quad \text{with } a_2 \text{ real} \tag{B.7}
$$

which has the solution

$$
\int e^{a_0 + a_1 v + a_2 v^2} dv = \int d\zeta = \zeta \tag{B.8}
$$

in the form of an indefinite integral with integration constants to be chosen for convenience. The scale factor is now

$$
h_v = \left|\frac{d\zeta}{dv}\right| = e^{\mathrm{Re}[a_0] - \mathrm{Im}[a_1]v_1 - a_2 v_1^2 + \mathrm{Re}[a_1]v_3 + a_2 v_3^2} \tag{B.9}
$$

which fits the required factored form. Writing

$$
\mathrm{Re}[a_0] = a_0' + a_0'' \quad \text{(each real)} \tag{B.10}
$$

we have

$$
\begin{aligned}
\frac{du_1}{dv_1} &= e^{2a_0' - 2\mathrm{Im}[a_1]v_1 - 2a_2 v_1^2} \\
\frac{du_3}{dv_3} &= e^{2a_0'' - 2\mathrm{Re}[a_1]v_3 - 2a_2 v_3^2}
\end{aligned}
\tag{B.11}
$$

which can be integrated to give indefinite integrals of the same form as (B.8) (now real). Here we have chosen the u_n to be positive monotonic functions of the respective v_n.

Appendix C. Reduction of General Class to Log-Spiral Solutions

There are some special cases of lenses belonging to the general class of solutions in Appendix B with $a_2 = 0$. For such cases it is convenient to introduce cylindrical (Ψ, ϕ, z) coordinates with the complex form

$$\begin{aligned} \zeta &= x + jy = \Psi e^{j\phi} \\ \ell n(\zeta) &= \ell n(\Psi) + j\phi \end{aligned} \tag{C.1}$$

Then the general solution in (B.8) becomes

$$\begin{aligned} \zeta &= \int_{v_0}^{v} e^{a_0 + a_1 v''} dv'' = e^{a_0} \left[\frac{1}{a_1} e^{a_1 v''} \right]_{v_0}^{v} \\ &= \frac{e^{a_0}}{a_1} \left[e^{a_1 v} - e^{a_1 v_0} \right] \end{aligned} \tag{C.2}$$

Here a_0 is not essential, giving merely a linear shift in v. The lower integration limit can be taken as ∞ with a phase angle such that $\mathrm{Re}[a_1 v_0] = -\infty$, giving our basic form of solution as

$$\begin{aligned} \zeta &= |a_1|^{-1} e^{a_1 v} \quad , \quad a_0 \equiv j \arg(a_1) \\ a_1 v &= \ell n(|a_1|\zeta) = \ell n(|a_1|\Psi) + j\phi \\ v &= a_1' \left[\ell n(|a_1|\Psi) + j\phi \right] = v_3 + j v_1 \\ a_1' &\equiv a_1^{-1} \end{aligned} \tag{C.3}$$

Note the choice of a_0 to remove an inconvenient shift in ϕ. Furthermore, $|a_1|^{-1}$ will have the dimensions of meters, a convenient distance scale. A convenient alternate form for the various constants is

$$\begin{aligned} a_1 &= a e^{ja'} \quad , \quad a, a' \text{ real} \\ a_1' &= a_1^{-1} = a^{-1} e^{-ja'} \\ |a_1| &= a \quad , \quad \arg(a_1) = a' = -j a_0 \\ \mathrm{Re}[a_1] &= a \cos(a') \quad , \quad \mathrm{Im}[a_1] = a \sin(a') \\ \mathrm{Re}[a_1'] &= a^{-1} \cos(a') \quad , \quad \mathrm{Im}[a_1'] = -a^{-1} \sin(a') \end{aligned} \tag{C.4}$$

The separate v_n coordinates are

$$
\begin{aligned}
v_1 &= \mathrm{Im}[a_1']\ell n(a\Psi) + \mathrm{Re}[a_1']\phi \\
&= a^{-1}\left[-\sin(a')\ell n(a\Psi) + \cos(a')\phi\right] \\
v_3 &= \mathrm{Re}[a_1']\ell n(a\Psi) - \mathrm{Im}[a_1']\phi \\
&= a^{-1}\left[\cos(a')\ell n(a\Psi) + \sin(a')\phi\right]
\end{aligned}
\tag{C.5}
$$

The perfectly conducting sheets are placed on boundaries of constant v_1, say $v_1^{(1)}$ and $v_1^{(2)}$, where such boundaries can be found from

$$
\Psi = a^{-1}e^{-\csc(a')av_1 + \cot(a')\phi} \tag{C.6}
$$

By appropriate choices of a and a' various logarithmic spirals can be produced.

For the u_n coordinates we first have

$$
\begin{aligned}
h_v &= \left|\frac{d\zeta}{dv}\right| = \left|e^{a_1 v}\right| = |a_1\zeta| = a\Psi \\
&= \left|e^{a_0 + a_1 v}\right| = e^{-\sin(a')av_1 + \cos(a')av_3}
\end{aligned}
\tag{C.7}
$$

Choosing the propagation coordinate u_3 first we have (from (B.2))

$$
\begin{aligned}
\frac{du_3}{dv_3} &= e^{2\cos(a')av_3} \\
u_3 &= \frac{\sec(a')}{2a}e^{2\cos(a')av_3} \\
&= \frac{\sec(a')}{2a}e^{2\cos^2(a')\ell n(a\Psi) + 2\cos(a')\sin(a')\phi}
\end{aligned}
\tag{C.8}
$$

with integration constant chosen for convenience. The remaining coordinate is then

$$
\begin{aligned}
\frac{du_1}{dv_1} &= e^{-2\sin(a')av_1} \\
u_1 &= -\frac{\csc(a')}{2a}e^{-2\sin(a')av_1} \\
&= -\frac{\csc(a')}{2a}e^{2\sin^2(a')\ell n(a\Psi) - 2\cos(a')\sin(a')\phi}
\end{aligned}
\tag{C.9}
$$

with integration constant again chosen for convenience.

The permittivity is now given by

$$\varepsilon = \frac{h_1}{h_3}\varepsilon_{\min} = \frac{\left|\frac{dv_1}{du_1}\right|h_v}{\left|\frac{dv_3}{du_3}\right|h_v} = \left|\frac{dv_3}{du_3}\right|\left|\frac{dv_1}{du_1}\right|$$

$$= e^{2\sin(a')av_1 + 2\cos(a')av_3} \qquad \text{(C.10)}$$

$$= e^{2\left[-\sin^2(a')+\cos^2(a')\right]\ell n(a\Psi)+4\cos(a')\sin(a')\phi}$$

$$= e^{2\cos(2a')\ell n(a\Psi)+2\sin(2a')\phi}$$

With this for ε, and (C.6) with boundaries $v_1^{(1)}$ and $v_1^{(2)}$ specified (or equivalently from (C.9) with $u_1^{(1)}$ and $u_1^{(2)}$ specified), we have the lens design equations. Parameters a and a' are available for us to choose at our convenience.

Appendix D. Two Simple Special Cases

The log-spiral solutions in Appendix C have special simpler cases. The case that $a' = \pi/2$ corresponds to a case in [2,3] in which

$$v_1 = -a^{-1}\ell n(a\Psi) \quad , \quad v_3 = a^{-1}\phi$$
$$u_1 = -\frac{e^{-2av_1}}{2a} = -\frac{\Psi^{-2}}{2a} \tag{D.1}$$
$$\frac{du_3}{dv_3} = 1 \quad , \quad u_3 = v_3 = a^{-1}\phi$$

Note in (C.8) that u_3 is singular; this can be avoided as above or by taking an appropriate limit and removing the irrelevant singular term. This solution applies to the case of an E-plane bend with circular cylindrical conducting sheets on cylindrical radii Ψ of Ψ_1 and Ψ_2 with

$$u_1^{(1)} = -\frac{\Psi_{max}}{2\Psi_1^2} \quad , \quad u_1^{(2)} = -\frac{\Psi_{max}}{2\Psi_2^2} \tag{D.2}$$
$$\Psi_{max} \equiv a^{-1} \equiv \text{maximum cylindrical radius of interest}$$

The permittivity for this case is

$$\varepsilon = \left(\frac{\Psi_{max}}{\Psi}\right)^2 \varepsilon_{min} \geq \varepsilon_{min} \tag{D.3}$$

This case is studied in more detail and illustrated in [2, 3].

Another simple case is given by $a' = 0$ for which

$$v_1 = a^{-1}\phi \quad , \quad v_3 = a^{-1}\ell n(a\Psi)$$
$$u_3 = \frac{a}{2}\Psi^2 \tag{D.4}$$
$$\frac{du_1}{dv_1} = 1 \quad , \quad u_1 = v_1 = a^{-1}\phi$$

Now in (C.8) we have u_1 singular; this is avoided in the same way as the previous example. This solution applies to the case of a radially expanding wave in an angular sector between perfectly conducting planar sheets on angles ϕ of ϕ_1 and ϕ_2 with

$$u_1^{(1)} = \Psi_{min}\phi_1 \quad , \quad u_1^{(2)} = \Psi_{min}\phi_2 \tag{D.5}$$
$$\Psi_{min} \equiv a^{-1} \equiv \text{minimum cylindrical radius of interest}$$

The permittivity for this case is

$$\varepsilon = \left(\frac{\Psi}{\Psi_{min}}\right)^2 \varepsilon_{min} \geq \varepsilon_{min} \tag{D.6}$$

this case is like a dual of the previous case is that the roles of the Ψ and ϕ coordinates and boundaries of the lends domain are interchanged. The geometry is then like the illustrations in [2,3] with this new interpretation.

References

1. C.E. Baum, Wedge Dielectric Lenses for TEM Waves Between Parallel Plates, Sensor and Simulation Note 332, September 1991.

2. C.E. Baum, Two-Dimensional Inhomogeneous Dielectric Lenses for E-Plane Bends of TEM Waves Guided Between Perfectly Conducting Sheets, Sensor and Simulation Note 388, October 1995.

3. C.E. Baum, Dielectric Body-of-Revolution Lenses with Azimuthal Propagation, Sensor and Simulation Note 393, March 1996.

4. C.E. Baum, Dielectric Jackets as Lenses and Application to Generalized Coaxes and Bends in Coaxial Cables, Sensor and Simulation Note 394, March 1996.

5. C.E. Baum and A.P. Stone, *Transient Lens Synthesis: Differential Geometry in Electromagnetic Theory*, Hemisphere Publishing Corp. (Taylor & Francis), 1991.